



ISSN: 0067-2904

Application of a Vegetation Health Index to Identify Distribution of Agricultural Drought in Diyala Province, Iraq

Rana S. Hadid, Bushra A. Ahmed

Remote Sensing and GIS Department, College of Science, University of Baghdad, Baghdad, Iraq

Received: 29/9/2023

Accepted: 4/2/2024

Published: 28/2/2025

Abstract

Over two decades, this study analyzes drought trends in Diyala Province, Iraq, and It utilizes remote sensing data and rainfall analysis to evaluate the severity and frequency of drought in 2002, 2005, 2010, 2015, 2020, and 2022. The research maps drought distributions in Diyala Province using satellite images from Landsat 7, Landsat 8, and Landsat 9 and analyzes the vegetation health index (VHI), soil moisture index (SMI), and average rainfall data. Results showed increased drought intensity: severe drought expanded from 48% in 2005 to 50% in 2022, and arid conditions increased from 1.1% in 2002 to 17.1% in 2022, as per SMI. Moreover, rainfall analysis reveals varying patterns, with 2022 experiencing lower average rainfall (4.215 mm) and higher variability (1.4633 mm standard deviation) compared to 2015 (6.735 mm, 1.1227 mm). The discoveries, pivotal for agriculture and water management, underscore the necessity of consistent monitoring and adaptable strategies for addressing shifting climate patterns.

Keywords: Agricultural Drought, Remote sensing, VHI, SMI, Google Earth Engine.

تطبيق مؤشر صحة الغطاء النباتي لتحديد توزيع الجفاف الزراعي في محافظة ديالى، العراق

رنا حديد، بشرى علي احمد

قسم التحسس النائي ونظم المعلومات الجغرافية، كلية العلوم، جامعة بغداد، بغداد، العراق

الخلاصة

يحلل هذا البحث اتجاهات الجفاف في محافظة ديالى بالعراق على مدى عقدين من الزمن ويستخدم بيانات الاستشعار عن بعد وتحليل هطول الأمطار لتقييم شدة وتواتر الجفاف في أعوام 2002 و 2005 و 2010 و 2015 و 2020 و 2022. يقوم البحث بعمل خرائط لتوزيع الجفاف في محافظة ديالى باستخدام صور الأقمار الصناعية من Landsat 7 و Landsat 8 و Landsat 9، ويحلل مؤشر صحة الغطاء النباتي (VHI) ومؤشر رطوبة التربة (SMI) و بيانات متوسط هطول الأمطار.. تُظهر النتائج زيادة في شدة الجفاف: حيث اتسعت مساحة الجفاف الشديد من 48% (2005) إلى 50% (2022)، وارتفعت شدة الجفاف من 1.1% (2002) إلى 17.1% (2022) وفقاً لـ SMI. يكشف تحليل هطول الأمطار عن أنماط مختلفة، حيث شهد عام 2022 هطولاً أقل من متوسط هطول الأمطار (4.215 ملم) وزيادة في التباين (1.4633 ملم من الانحراف المعياري) مقارنة بعام 2015 (6.735 ملم، 1.1227 ملم). تسلط هذه النتائج، التي تعتبر حاسمة لقطاعي الزراعة وإدارة المياه، الضوء على الحاجة إلى الرصد المستمر ووضع استراتيجيات تكيفية استجابةً لنماذج مناخية متغيرة.

1. Introduction

Drought is a natural climatological phenomenon that occurs due to a shortage of rainfall in an area. The manifestation of this in agriculture is a shortage of water supply to meet crop water requirements, whether from rainfall or irrigation [1]. Drought can be classified into four types: meteorological, agricultural, hydrological, and socio-economic [2]. Meteorological drought occurs when there is a deficit between precipitation and evaporation; agricultural drought is determined by soil moisture and plant characteristics, while hydrological drought occurs when river flow or aquifer water levels drop below average. Socio-economic drought refers to the relationship between the water supply and demand. Vegetation is sensitive to the effects of drought, which can lead to a decrease in water availability and a deterioration in its condition [3]. Agricultural drought is a highly complex natural hazard that challenges monitoring and prediction. It has far-reaching effects, impacting vast areas and substantially reducing food production. Monitoring and predicting agricultural drought accurately is crucial for implementing timely mitigation measures and ensuring food security [4].

Iraq is located in the driest region in the world, with limited water resources shared with neighboring countries. Water is vital for the stability and development of the agricultural sector and the economy, which relies heavily on surface and groundwater resources; despite this, Iraq has experienced repeated droughts over the past two decades [5].

The climate is classified based on the climatic elements of rainfall, temperature, humidity, and wind, which determine the characteristics of each climate type. Climate classification groups the world's climates based on different climate factors, such as rainfall, temperature, humidity, and wind. It is used to identify the characteristics of each climate type and to correlate them with biomes, which are areas with similar plant and animal life. One of the most widely used climate classification systems is the Köppen climate classification scheme, which divides climates into five main groups: A (tropical), B (arid): Low precipitation, with less than 10 inches per year, C (temperate), D (continental), E (polar), in the study area is climate classified to BWh: Hot desert climate, and BSh: Hot semi-arid climate. The study area is experiencing the effects of global climate change, as evidenced by rising temperatures, evaporation, declining rainfall, and relative humidity from 2001 to 2025 (Figure 1 [6], [7]).

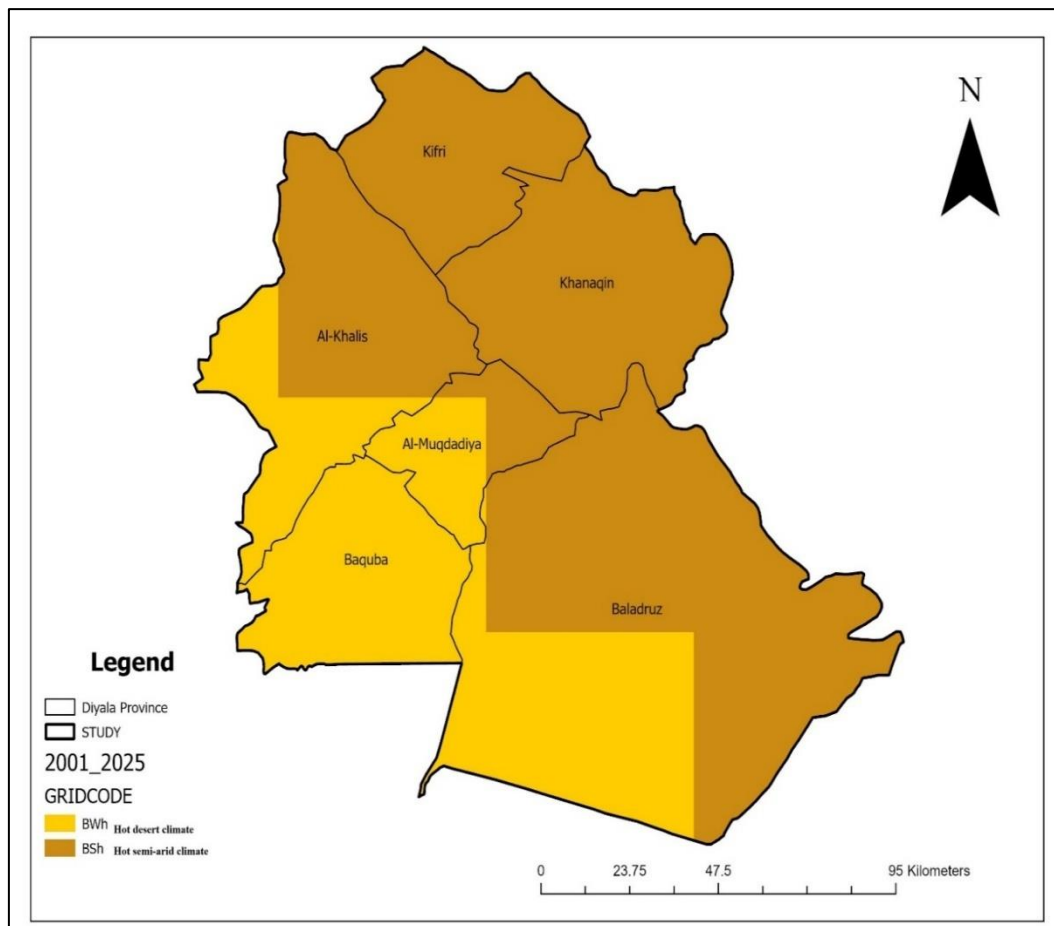


Figure 1: Köppen climate classification map for Diyala province during 2001-2025, [6], [7].

Decision-makers in many countries are currently utilizing remote sensing technology to bridge the information gap in drought monitoring. Remote sensing data from satellite sensors offers continuous datasets valuable for detecting the onset, duration, and severity of drought events. Compared to traditional methods, remote sensing is a superior tool for monitoring and issuing early warnings regarding drought. However, a challenge in utilizing remote sensing data for drought monitoring lies in validating and calibrating different indices to suit the specific ecological conditions and regions of interest [8].

Several drought indices have been developed and applied using remote sensing, including duration, intensity, severity, and spatial extent. The Normalized Difference Vegetation Index (NDVI) is a widely used approach for monitoring drought events by examining vegetation health. Combining NDVI with temperature has proven to be an effective way to improve the approach. The combination of NDVI and LST provides a strong correlation and valuable information for the early detection of agricultural drought as an early warning system [9]. The Vegetation Health Index (VHI) is an index that combines NDVI and LST to assess the impact of moisture and temperature on vegetation. It has been used to monitor and analyze conditions during drought events [10]. Drought significantly affects plants and wildlife, as water scarcity leads to a decline in plant health and growth capacity. Moreover, drought results in water resource depletion and affects the ecological balance.

Numerous researchers have conducted extensive research on drought and vegetation indices in different regions of Iraq. Previous studies have focused on comprehending drought using various indicators, including drought duration, intensity, spatial impact, and temporal

patterns. Recent findings propose combining indicators such as the NDVI with temperature data can contribute to early drought detection. For example, A study by **A. M. Saleh 2015 [11]** developed an algorithm for obtaining LST and Land Surface Emissivity (LSE) in Mosul City, Iraq, using Landsat-8 data. The algorithm used the Split-Window (SW) approach, utilizing brightness temperature values from bands 10 and 11. The NDVI threshold was used to differentiate between bare soil and vegetated areas, and fractional vegetation cover (FVC) was derived. The study found that 30.66% of the total area is under vegetation land cover, while 28.97% is under hilly regions. The SW algorithm proved a suitable and robust method for obtaining LST maps from Landsat-8 satellite data.

Another study by **H.A.A. Gaznyee et al. 2021[3]** analyzed drought severity in ten districts of Erbil governorate, Iraq, over 20 years (1998-2017). Their results showed frequent droughts, with extreme VCI-based drought areas recorded in 1999, 2000, 2008, and 2011, respectively. The highest crop yield reduction occurred in 2000, 2008, and 2012 due to low precipitation rates. The study highlights the VCI's ability to predict drought characteristics and its relationships with ecological variables, providing crucial information for decision-makers in environmental and economic sectors.

R.S. Hameed et al.2021 [12] proposed a new vegetation index called the normalized difference vegetation shortwave index (NDVSI). The NDVSI was less sensitive to atmospheric effects than the NDVI. It is calculated by dividing the difference between the sum of the NIR and SWIR cubic bands. SAVI and NDVSI ($R^2 = 0.809$) and NDVI and NDVSI ($R^2 = 0.917$) showed strong correlations in the study, indicating that NDVSI can be used as a stand-alone vegetation index for vegetation identification.

M. F. Allawai et al. 2020 [13] focused on the changes in land cover in Mosul Province, Iraq, from 2014 to 2018 using Geographic Information Systems (GIS) and remote sensing techniques. Satellite images from Landsat 8 were used to measure the NDVI and the Green Normalized Difference Vegetation Index (GNDVI). The results show a decrease in vegetation cover from 4.98% in 2014 to 4.39% in 2018. Water levels decreased by 0.4%, 0.38%, 0.27%, 0.48%, and 0.28% for the same period. Urban area decreased by 16.02–10.92% between 2014 and 2016, but reconstruction increased. NDVI and GNDVI are good indicators for vegetation and land use/cover changes, with NDVI showing a more significant increase in vegetation due to increased water use. Their study highlights the importance of NDVI as an indicator of vegetation-moisture conditions in Mosul Province.

H. A. Atiyah et al. 2023 [14] conducted a study investigating drought and vegetation indices using remote sensing data in Babel Province. The results indicated similar drought conditions in 2015 and 2018 based on NDVI analysis. However, in 2021, the SPI values suggest a more severe drought. Additionally, there was a 9% decrease in the vegetation area in 2021 compared to previous years. These findings hold importance for government planners in effectively managing the impacts of drought in the region.

The study aimed to identify the distribution of agricultural drought in Diyala Province using the VHI. The research used a long-term sequence of dry and wet season Landsat data from 2002, 2005, 2010, 2015, 2020, and 2022 to derive VHI. Landsat data was selected due to its open-access policy and acceptable temporal and spatial resolution for drought monitoring. The Google Earth Engine (GEE) [15], an open-source platform for time-series analysis and large-scale application, is adopted to design the Vegetation index-based approach and release the spatiotemporal products. The Google Earth Engine offers georeferenced and atmospherically corrected real-time remote; it combines remote sensing data, including satellite imagery from various sources, with high-performance computer service, making satellite imagery processing quicker and simpler. The GEE uses JavaScript for client libraries and Python for code modification. It employs Map reduce architecture for parallel processing, dividing large volumes of data into smaller sets and assembling output datasets after

processing them as individual components [16]. The study's results showed the region's spatial and temporal distribution of agricultural drought, providing valuable information for drought management and mitigation efforts.

2. Materials and Methods

Understanding the distribution of agricultural drought in Diyala Province, Iraq, is crucial for informing water management strategies and ensuring the long-term sustainability of the region's agricultural sector. This study leverages remote sensing data and rainfall analysis to assess drought severity and frequency over twenty years, providing intervals (2002, 2005, 2010, 2015, 2020, and 2022), Figure 2. Through the calculation of various vegetation indices, including NDVI, LST, VCI (Vegetation Condition Index), TCI (Temperature Condition Index), SMI (Soil Moisture Index), and VHI (Vegetation Health Index), alongside the analysis of precipitation patterns, this study sheds light on the temporal and spatial dynamics of agricultural drought in Diyala Province.

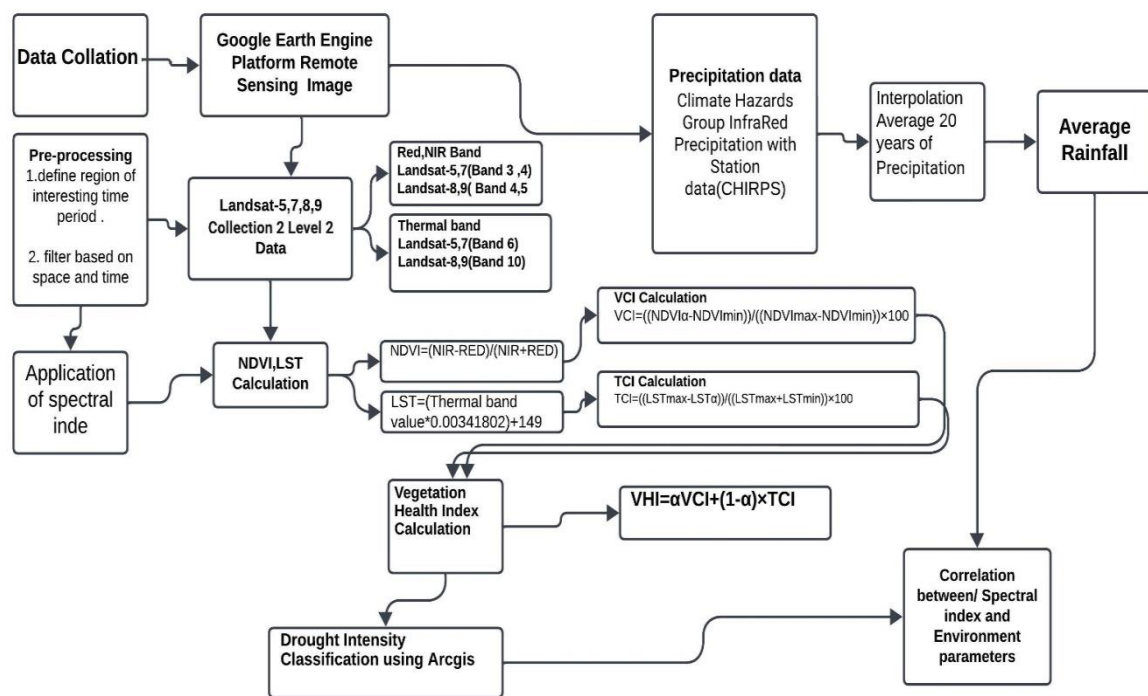


Figure 2: Methodology flowchart for VHI and Rainfall calculation with Google Earth Engine.

2.1. Study Area

Diyala province is situated in the northeastern region of Iraq, at 33° latitudes and 35° N and longitudes 45° and 46° E. It spans approximately 17.685 km² [17] (Figure 3). The study area has a unique transitional climate due to its location within two distinct regions: semi-mountainous and sedimentary. This combination results in a climate that blends characteristics of arid and semi-arid regions. The province experiences high summer temperatures surpassing 40°C and low winter temperatures with limited rainfall [18]. The climatic variations pose challenges for the agricultural sector, emphasizing the importance of implementing effective drought monitoring and management strategies in Diyala Province.

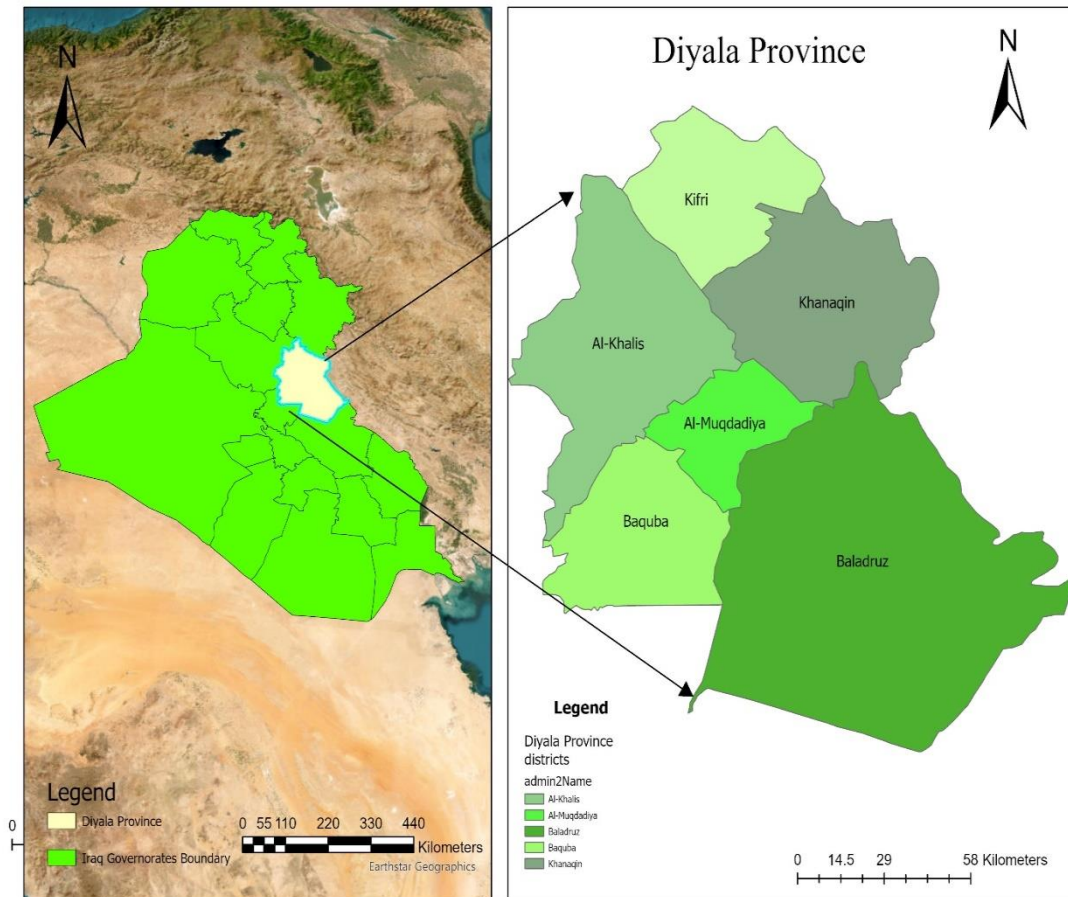


Figure 3: The study area is located in Diyala Province, Iraq

2.2. Remote Sensing Data

The study utilized two types of remote sensing data: Landsat images and rainfall data.

2.2.1. Landsat images

The study mapped drought distributions in Diyala Province in 2002, 2005, 2010, 2015, 2020, and 2022. The satellite images were acquired by Landsat 7, Landsat 8, and Landsat 9, which are more than 20 years. The sensors used to acquire the images were the Enhanced Thematic Mapper Plus (ETM+), the Operational Land Imager (OLI), the Thermal Infrared Sensor (TIRS), OLI-2, and TIRS-2. New for Collection 2 is the processing and distribution of Level-2 surface reflectance and surface temperature science products for Landsat 7 ETM+ and Landsat 8 OLI/TIRS. Level-2 products are generated from Collection 2 Level-1 inputs that meet the Smaller than 76 degrees Solar Zenith Angle constraint and include the required auxiliary data. NDVI, LST was calculated using GEE, representing the data of (Path/row: 168/36, 168/37). Landsat images were obtained from January to December in 2002, 2005, 2010, 2015, 2020, and 2022 to estimate annual plant productivity in the study area.

2.2.2. Rainfall Data

Precipitation data were obtained from the Climate Hazards Infrared Precipitation with Stations (CHIRPS) dataset provided by the GEE. The study used monthly CHIRPS precipitation with a spatial resolution of 0.05° from 2002 to 2022. CHIRPS has the advantages of a long recording period from 1981 to the present, high spatial resolution, low spatial bias,

and low time delay [10], and has been recently applied in various fields in drought monitoring. CHIRPS is a 30+ year quasi-global rainfall dataset. CHIRPS incorporates 0.05° resolution satellite imagery with in-situ station data to create gridded rainfall time series for trend analysis and seasonal drought monitoring [19]. The study area's rainfall data were interpolated using Interpolation Distance Weighting (IDW) using rainfall values derived from CHIRPS data. Initially, the precipitation data from weather stations were transformed into shapefiles (point data). Subsequently, these shapefiles were interpolated into raster layers on ArcMap10.8 employing the IDW tool [20].

2.3. Drought index calculation

The study uses Landsat data to analyze the Vegetation Health Index using long-term sequence data for 2002, 2005, 2010, 2015, 2020, and 2022 mean annual. The satellite data is being used in the analysis to precisely measure how changes in the drought analysis affect NDVI, LST, and the VHI.

2.3.1. Normalized Difference Vegetation Index (NDVI) is an early vegetation index used to monitor drought, distinguish vegetation cover, and determine density, enabling accurate monitoring of land cover types [21]. Using the Red and NIR bands, the vegetation index determines how much energy is received and given off by objects on the earth, where Red is the visible red band and NIR [22]. To calculate NDVI, a digital number (DN) and different band values were used; these pixel bands produced a digital number value [23] (Figure 4). NDVI can be expressed by equation (1) [24]:

$$\text{NDVI} = \frac{\text{NIR} - \text{RED}}{\text{NIR} + \text{RED}} \quad (1)$$

Theoretically, NDVI values range from -1.0 to +1.0, but the typical range is -0.1 for non-vegetated surfaces and 0.9 for dense vegetation. NDVI values increase with green biomass, positive seasonal changes, and favorable factors like abundant precipitation [24].

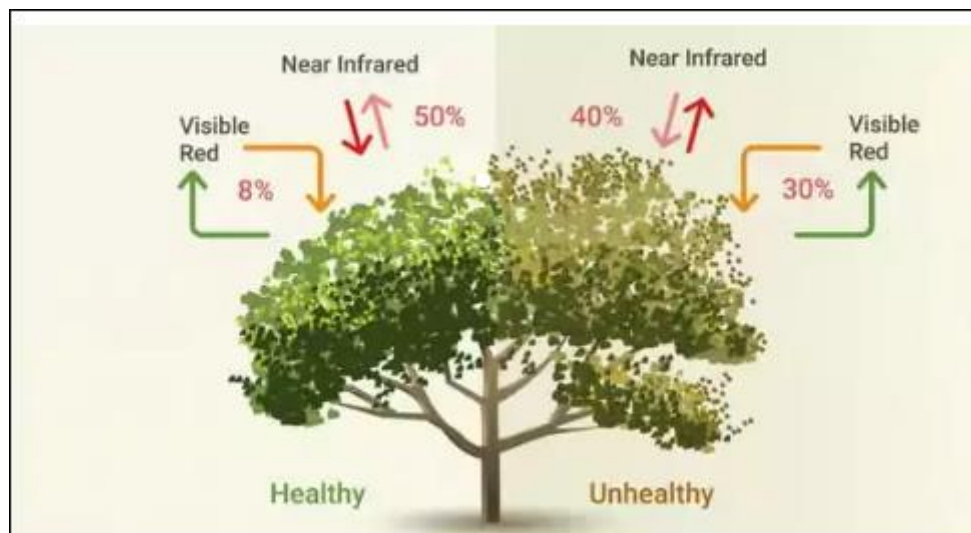


Figure 4: A Healthy plant (left) absorbs much visible light and reflects a large portion of near-infrared light. Unhealthy or sparse vegetation (right) absorbs more visible light and reflects less near-infrared light [23].

2.3.2. Land Surface Temperature (LST) can be measured when the instrument touches the surface [25]. LST information reveals temporal and spatial variations of the surface equilibrium state, crucial in various fields like evapotranspiration, climate change, hydrological cycles, vegetation monitoring, and environmental studies [11]. Landsat 4-7 and Landsat 8-9 use a single-channel algorithm to generate Surface Temperature (ST) products. The algorithm is derived from the RIT ST code. Collection 2 ST is obtained from thermal infrared bands, utilizing TOA Reflectance, TOA BT, ASTER GED data, ASTER NDVI data, and atmospheric profiles. For Landsat 7, Band 6 TOA BT combines 6H and 6L, replacing saturated 6H pixels with 6L [26]. Similarly, Landsat 8-9 ST product is derived from TIRS band 10, with the same algorithm and incorporating TOA Reflectance, TOA BT, ASTER GED data, ASTER NDVI data, and atmospheric profiles [27].

The equations to convert the thermal bands of Landsat 5-7 and Landsat 8-9 Surface Reflectance (L8SR) images to surface temperature and then convert from Kelvin to Celsius are as follows [28]:

1. Conversion equation for thermal bands:

$$LST = (\text{Thermal band value} * 0.00341802) + 149 \quad (2)$$

2. Conversion equation from Kelvin to Celsius:

$$LST(\text{Celsius}) = LST(\text{Kelvin}) - 273.15 \quad (3)$$

2.3.3. Soil Moisture Index (SMI)

The study uses the LST approach and NDVI to estimate soil moisture by reducing the soil moisture index and extracting vegetation density information. Vegetation cover significantly impacts soil moisture, with increasing cover depleting moisture content. Surface temperature is indicative of soil moisture levels [29].

The calculation for the SMI is as given by equation (4) [30][31]:

$$SMI = \frac{LST_{\max} - LST}{LST_{\max} - LST_{\min}} \quad (4)$$

LST_{max} and LST_{min} represent the highest and lowest surface temperature values corresponding to a specific NDVI value. LST refers to Land Surface Temperature, which is obtained from remote sensing data and represents the temperature of a pixel on the Earth's surface [30].

2.3.4. Vegetation and Temperature Condition Index and Vegetation Health Index

In order to estimate the thermal and humidity conditions of vegetation for each overlapping pixel, the following equations [32] can be used to calculate the temperature condition index (TCI) and vegetation condition index (VCI); the following Equations (5) and (6) [32]:

$$VCI = \frac{(NDVI_{\alpha} - NDVI_{\min})}{(NDVI_{\max} - NDVI_{\min})} \times 100 \quad (5)$$

$$TCI = \frac{(LST_{\max} - LST_{\alpha})}{(LST_{\max} + LST_{\min})} \times 100 \quad (6)$$

The VCI and TCI values range from 0-100 and indicate the vegetation and temperature environmental conditions. They are inversely related, meaning a higher VCI value corresponds to a lower TCI value. Combining the VCI and TCI values equally allows for calculating the VHI using Equation (7) [32].

$$VHI = \alpha VCI + (1 - \alpha) \times TCI \quad (7)$$

where $\alpha=0.5$ (contribution of VCI and TCI).

3.3.5. Drought Intensity Classification

Drought intensity was assessed by analyzing VHI values, where values below 40 represented drought areas and values above 40 indicated healthy vegetation. Drought regions below 40 were divided into mild, moderate, severe, and extreme categories based on specific VHI value ranges, Table 1 [33]. Area estimations determine the extent of these drought categories and non-drought areas, such as forests, agriculture regions, and water bodies. VHI values are lower for water bodies, resembling drought areas, because NDVI and LST values are typically low in water-covered regions [1].

Table 1: Classification scheme for drought mapping

Drought classes	VHI Values
Extreme drought	<10
Severe drought	10-20
Moderate drought	20-30
Mild drought	30-40
No drought	>40

3. Results and Discussions

The NDVI theoretically ranges from -1 to 1, where negative values indicate water, values around zero represent bare soil, and values closer to 1 reflect denser green vegetation. Figure 5 depicts the spatial distribution of NDVI in Diyala province for 2002, 2005, 2010, 2015, 2020, and 2022.

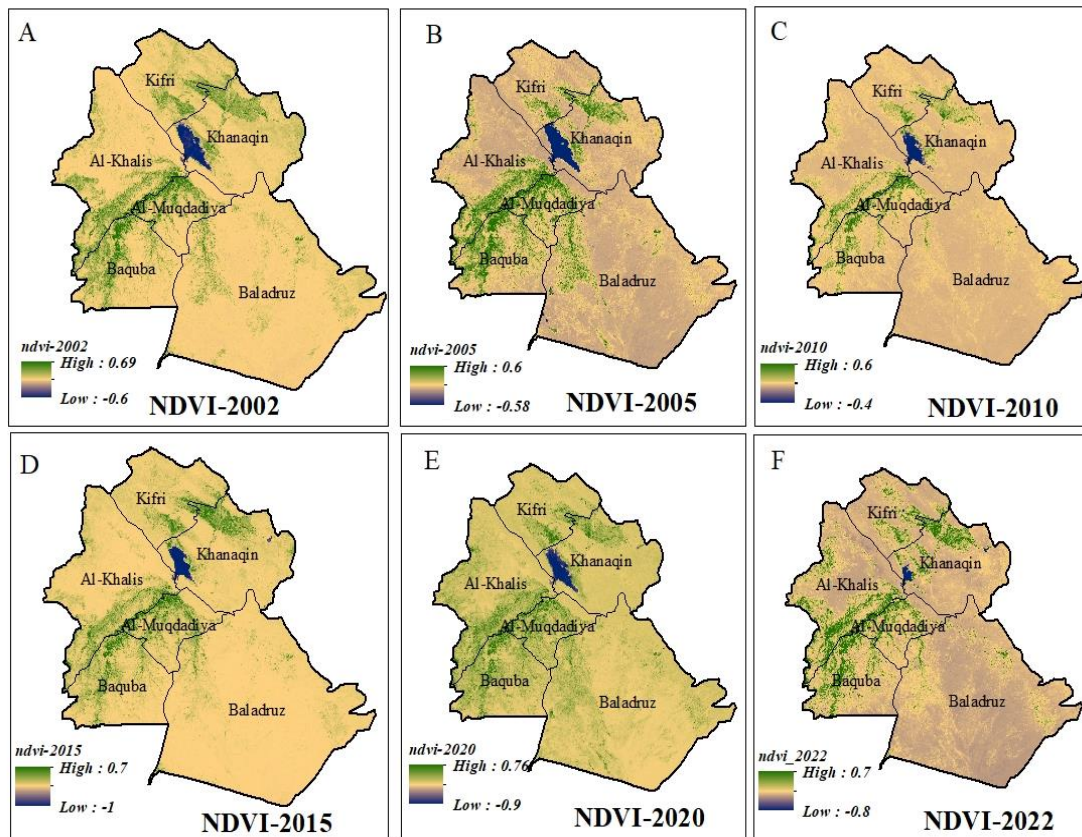


Figure 5: Spatial variation of NDVI for the years (a) 2002, (b) 2005, (c) 2010 and (d) 2015, (e)2020, (f)2022.

The LST of the study area reveals the spatial distribution of hot spots based on data from 2002, 2005, 2010, 2015, 2020, and 2022 (Figure 6). The LST was classified into two classes, low (ranging from 17°C to 23°C in 2002 and 2022, respectively) and high (ranging from 45°C to 66°C in 2005 and 2015, respectively).

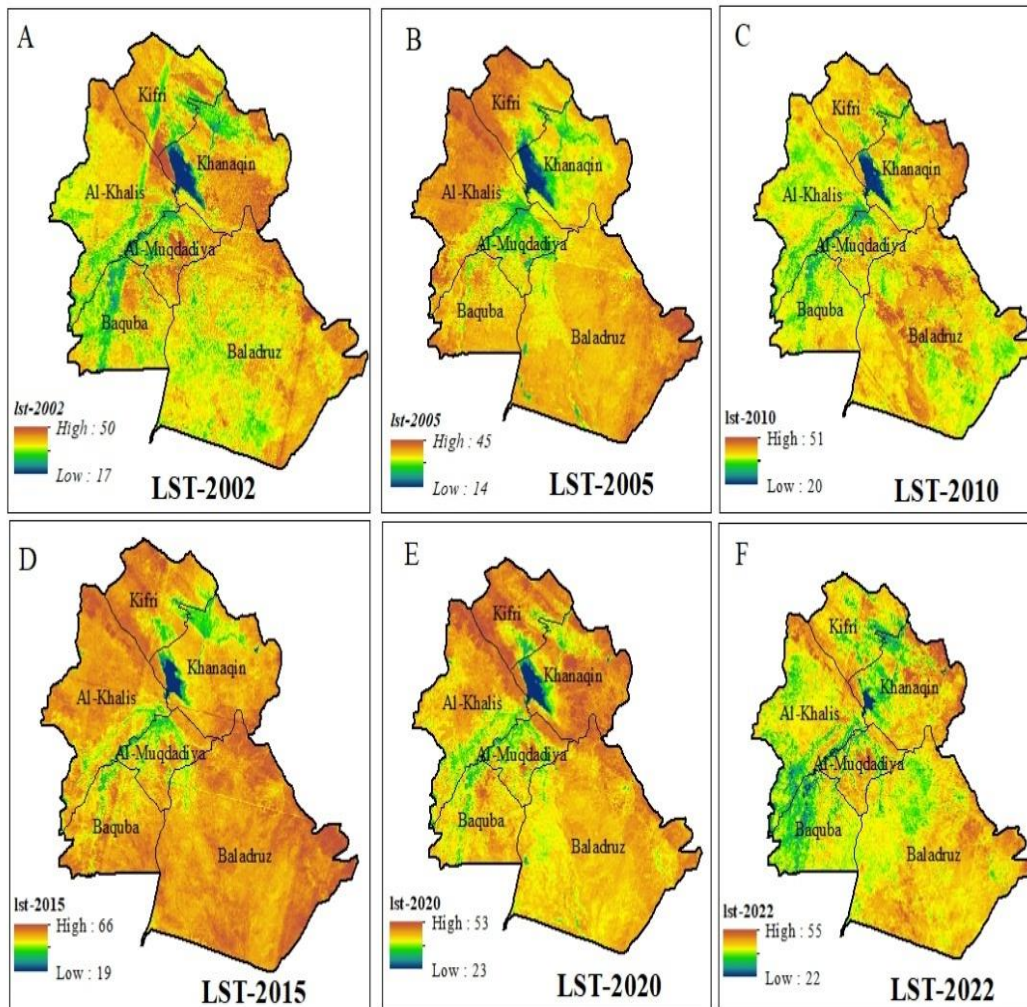


Figure 6: Spatial variation of LST for the years (a) 2002, (b) 2005, (c) 2010 and (d) 2015, (e)2020, (f)2022

The VCI and TCI range from 0 to 100, with higher values indicating more favorable environmental conditions for vegetation and lower temperatures, respectively. These indices exhibit an inverse relationship, meaning that as VCI increases, TCI decreases. Combining VCI and TCI values with equal weight results in the VHI. Figures 7 and 8 depict the spatial distribution of VCI and TCI in Diyala province for 2002, 2005, 2010, 2015, 2020, and 2022.

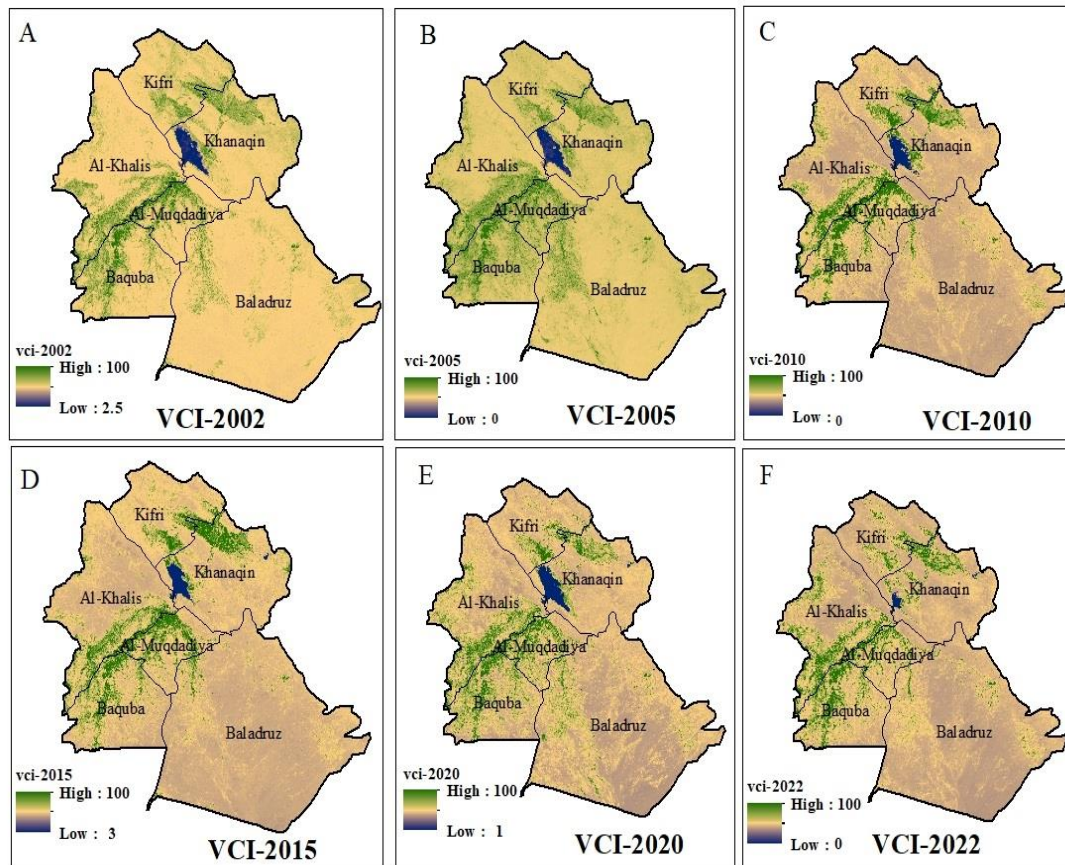


Figure 7: Variation in vegetation conditions index for the year (a) 2002, (b) 2005, (c) 2010 and (d) 2015, (e)2020, (f)2022

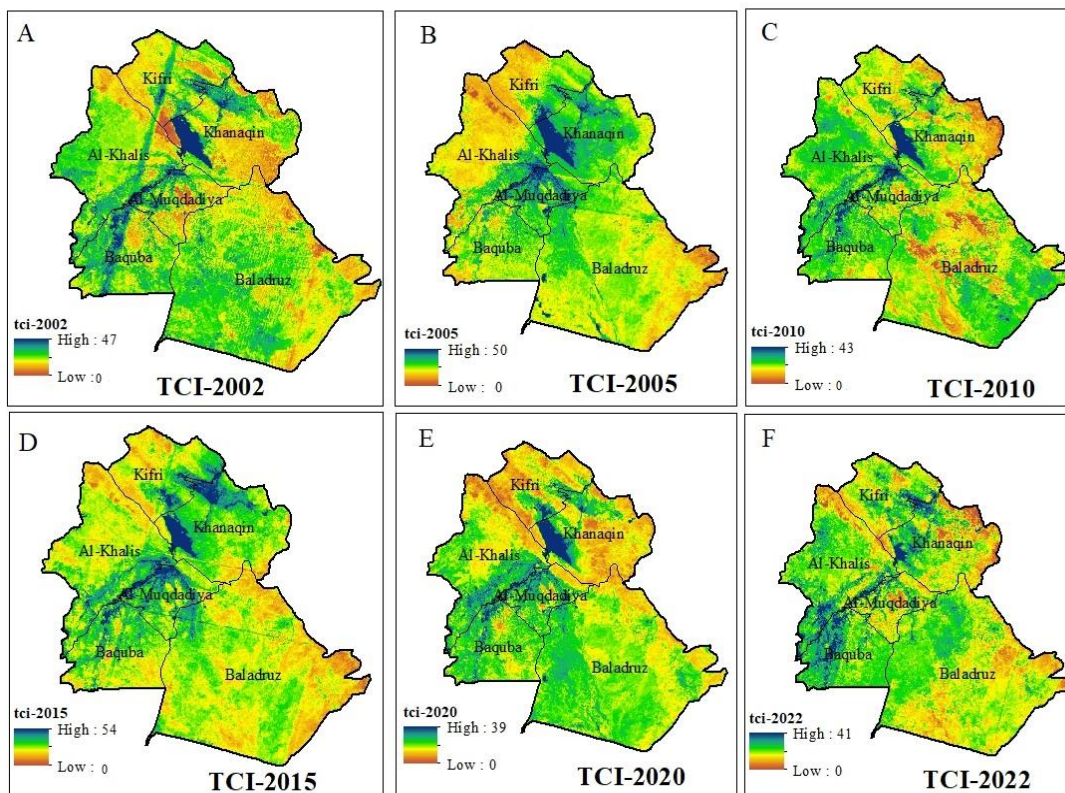


Figure 8: Variation in temperature conditions index for the year (a) 2002, (b) 2005, (c) 2010 and (d) 2015, (e)2020, (f)2022

3.1. Outcomes of the Vegetation Health Index (VHI)

Drought intensity was evaluated through VHI analysis, where values below 40 indicated drought-affected areas and values above 40 denoted healthy vegetation within drought-affected regions ($VHI < 40$). Further classifications were made based on specific VHI ranges for the years 2002 (20-70), 2005 (22-67), 2010 (19-68), 2015 (24-71), 2020 (17-65), and 2022 (18-66), Figure 9.

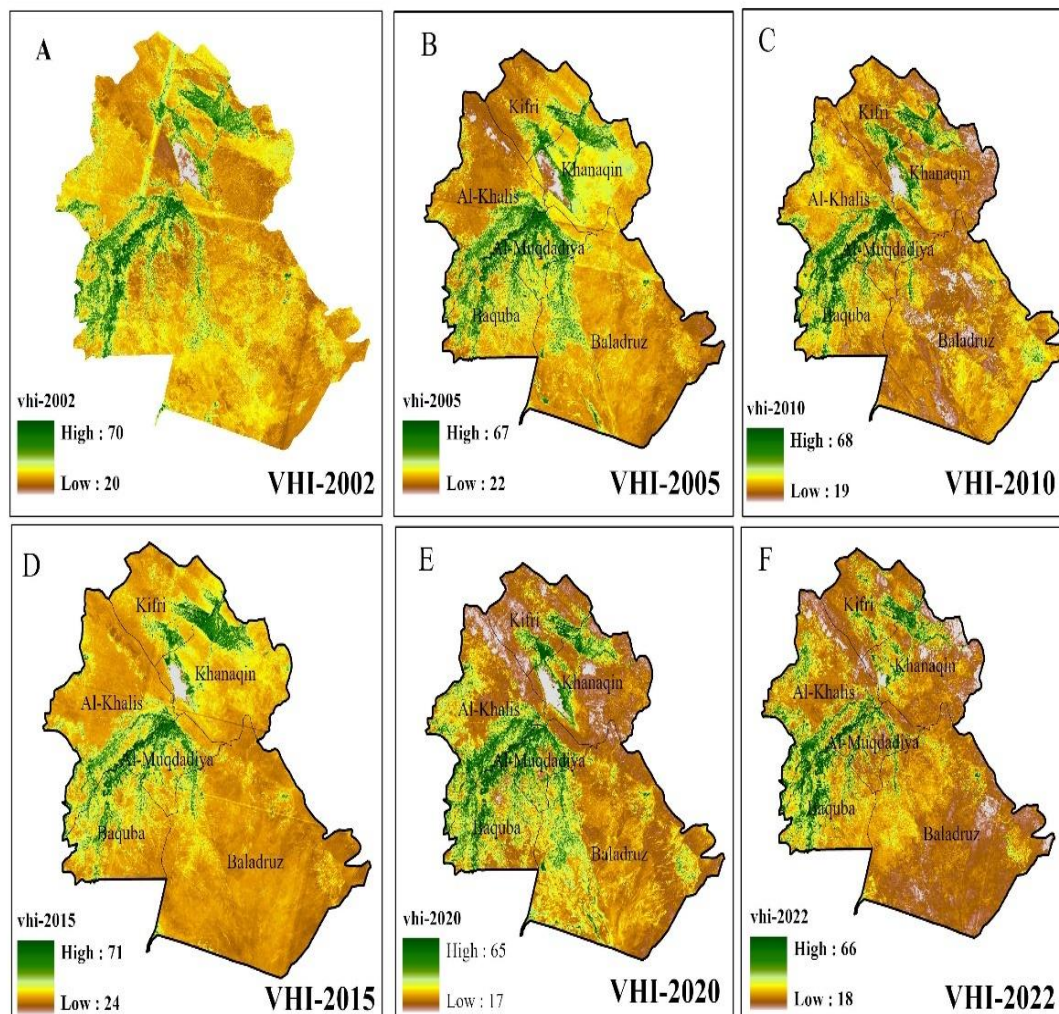


Figure 9: Spatial variation of VHI at (a) 2002, (b) 2005, (c) 2010 and (d) 2015, (e)2020, (f)2022

The study revealed changes in drought intensity in Diyala province over time, Table 2 and Figure 10. Moderate drought affected the most significant area, 134.266 ha (66%), in 2002, followed by mild drought, 51.680 ha (26%), and no drought in the remaining area 16.533 ha (8%). In 2005, severe drought decreased to 97.794 ha (48%), with moderate drought covering 65,647 ha (32%), mild drought covering 30,705 ha (15%), and the area without drought being 8,334 ha (4%). By 2010, severe drought covered 70,254 ha (35%), while moderate drought increased to 106,194 ha (52%), mild drought decreased to 20,172 ha (10%), and the area without drought was 5,860 ha (3%). In 2015, severe drought affected 73,858 ha (36%), followed by moderate drought with 78,956 ha (39%). In 2020, severe drought increased again, covering about 97,794 ha (48%), while moderate drought decreased to 65,647 ha (32%). Mild drought remained at 30,705 ha (15%), and the area without drought was 8,334 ha (4%). The most recent data in 2022 showed a similar pattern, with severe drought covering 100,760 ha

(50%), moderate drought affecting 73,956 ha (37%), mild drought covering 21,504 ha (11%), and the area without drought being 6,260 ha (3%).

Table 2: Extent of agricultural drought in 2002, 2005, 2010, 2015, 2020, and 2022

	2002		2005		2010	
Level of Drought	Area(ha)	Percent	Area(ha)	Percent	Area(ha)	Percent
Severe drought	-----	-----	97.794	48	70.254	35
Moderate drought	134.266	66	65.647	32	106.194	52
Mild drought	51.680	26	30.705	15	20.172	10
No drought	16.533	8	8.334	4	5.860	3
	2015		2020		2022	
Level of Drought	Area (ha)	Percent	Area(ha)	Percent	Area(ha)	Percent
Severe drought	73.858	36	97.794	48	100.760	50
Moderate drought	78.956	39	65.647	32	73.956	37
Mild drought	21.277	11	30.705	15	21.504	11
No drought	28.388	14	8.334	4	6.260	3

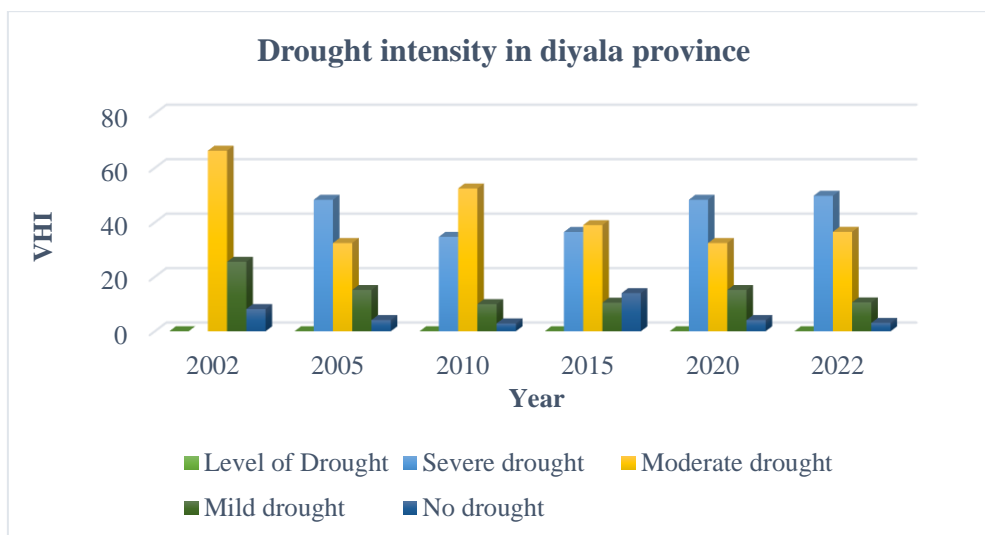


Figure10 :Drought Intensity in Diyala Province in 2002, 2005, 2010, 2015, 2020, and 2022

3.2. Outcomes of the Soil Moisture Index (SMI)

In Diyala Province, there has been an overall shift towards drier conditions over the last two decades, Table 3. The proportion of arid areas rose from 1.1% in 2002 to 17.1% in 2022, while the percentage of wet areas declined from 2.4% in 2002 to 0.8% in 2022, Figures 11 and 12.

Table 3 : Soil Moisture Index values for each year in Diyala Province

Year	2002	2005	2010	2015	2020	2022
SMI values	%	%	%	%	%	%
Arid conditions	1.1	2.1	0.4	5.9	12.9	17.1
Dry conditions	66.7	49.7	43.1	76.0	65.9	41.2
Moderate conditions	28.5	45.0	40.5	14.8	18.3	31.7
Wet conditions	2.4	2.3	14.4	2.5	1.8	9.2
Very wet conditions	1.3	1.0	1.6	0.8	1.0	0.8

These trends in soil moisture conditions indicate the varying levels of moisture availability over the years. The increase in arid conditions and the decrease in dry conditions in recent years highlight the potential impact of changing climate patterns on soil moisture availability.

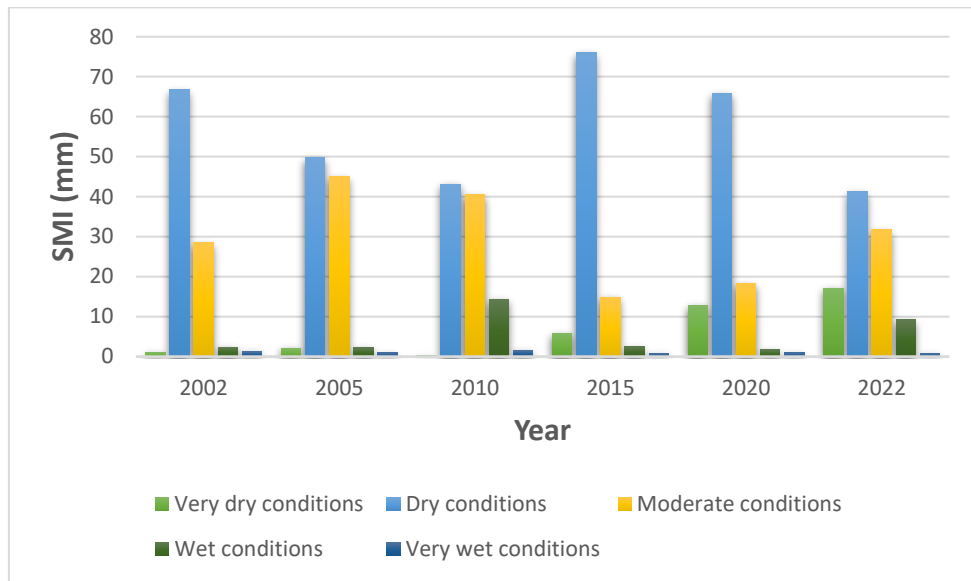


Figure 11: Soil moisture in Diyala province in 2002,2005,2010, 2015,2020 and 2022

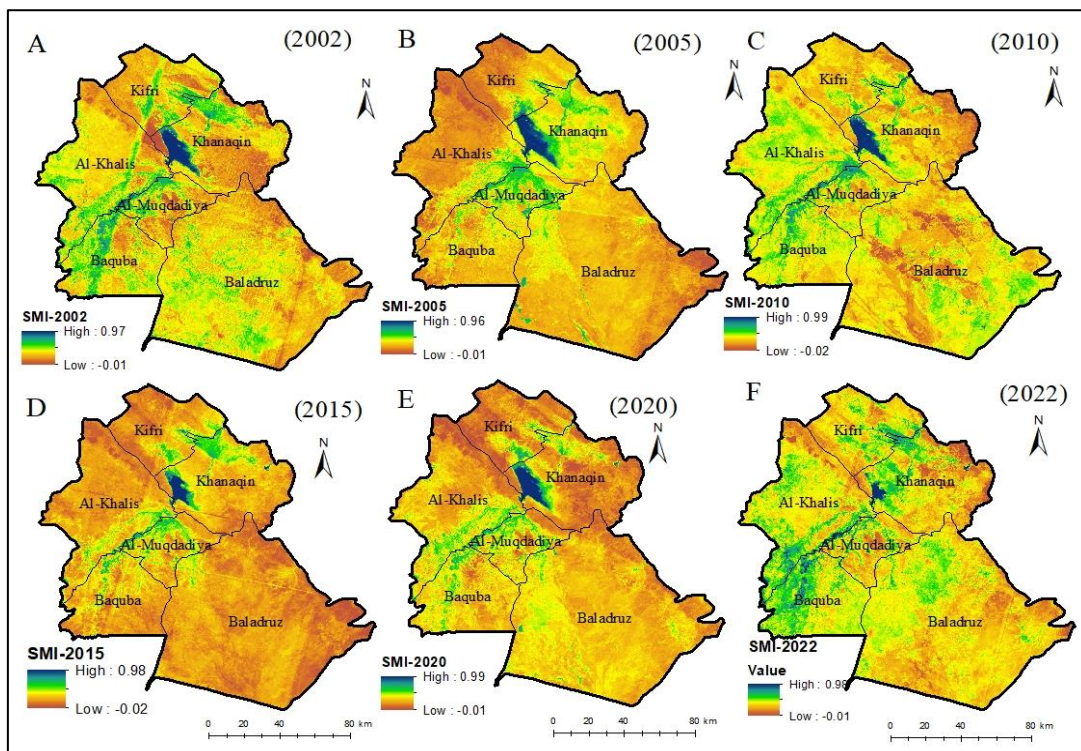


Figure 12: Spatial variation of Soil Moisture Index (SMI) mapping for (a) 2002, (b) 2005, (c) 2010, (d) 2015, (e)2020, and (f) 2022

3.3. Outcomes of the Average Rainfall

The study comprehensively analyzes the average annual rainfall through a time series complemented by spatial analysis maps. These maps reveal varying patterns in rainfall distribution over different years, showcasing notably low rainfall that suggests potential

drought periods, juxtaposed with years marked by higher precipitation levels, Figures 13 and 14.

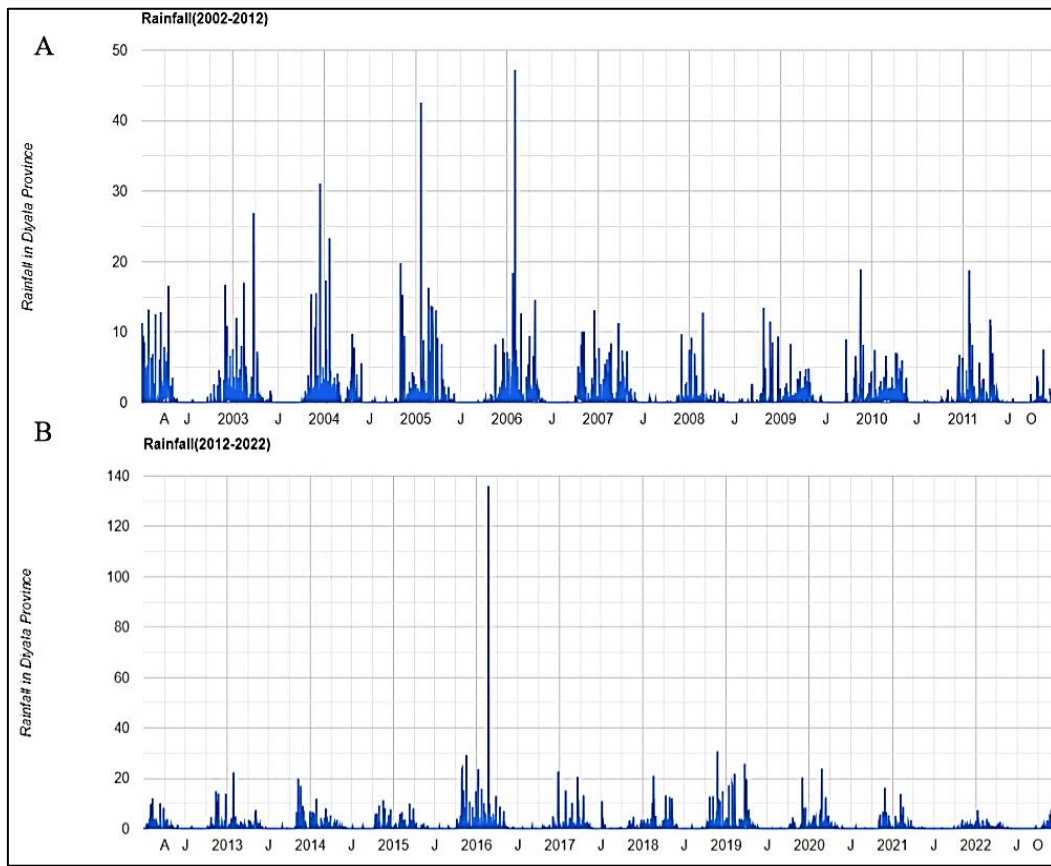


Figure 13: Annual Average Rainfall chart for (a)2002-2012, (b) 2012-2022 in Diyala Province

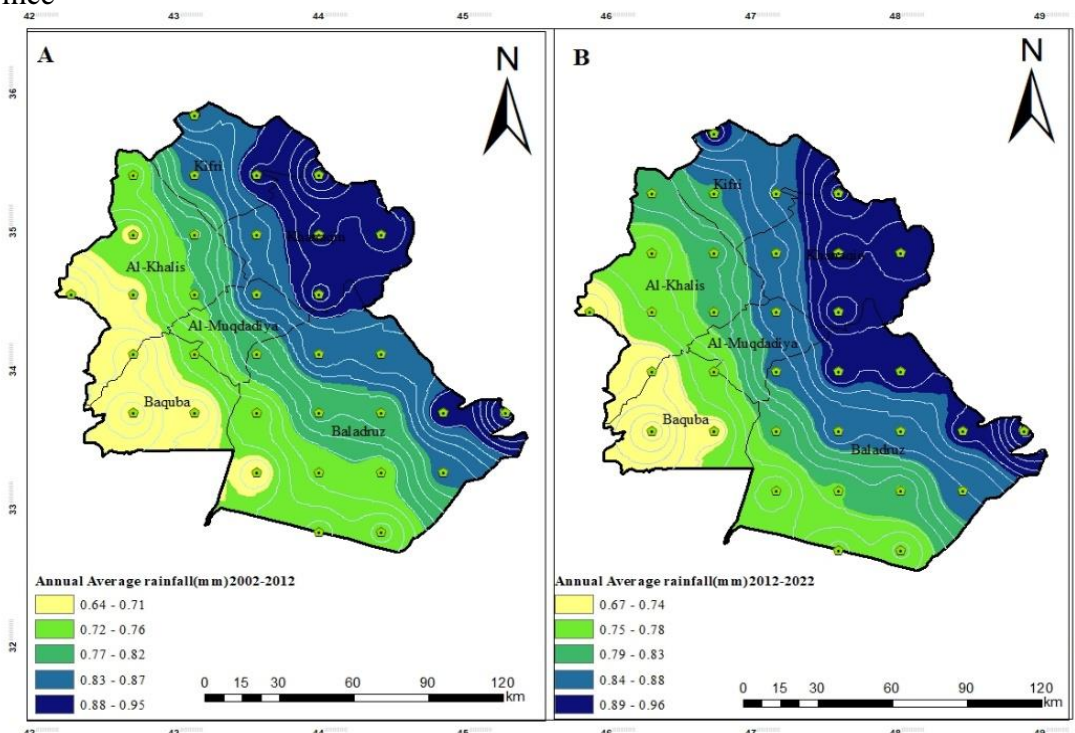


Figure 14: Spatial analysis map for Annual average rainfall for (a)2002-2012 and (b) 2012-2022 in Diyala Province

Analyzing the standard deviation (SD) of annual rainfall for 2002, 2005, 2010, 2015, 2020, and 2022 helped us understand how drought intensity has changed. Higher (SD) values signify increased fluctuations in rainfall, potentially indicating variable drought conditions, as outlined in Table 4 and Figures (15- 22). These values offer insights into both the average rainfall and rainfall variability (standard deviation) in Diyala province across specific years. For instance, in 2022, the province witnessed a lower average rainfall of 4.215 mm, accompanied by higher rainfall variability, with a standard deviation of 1.4633 mm. Conversely, in 2015, the province experienced a higher average rainfall of 6.735 mm, yet the rainfall exhibited greater consistency with a standard deviation of 1.1227 mm.

Table 4 Average rainfall and standard deviation for 2002, 2005, 2010, 2015, 2020, and 2022

Year	Average Rainfall (mm)	Standard Deviation (mm)
2002	5.744	0.2536
2005	6.660	0.9811
2010	5.334	0.3441
2015	6.735	1.1227
2020	5.413	0.1239
2022	4.215	1.4633

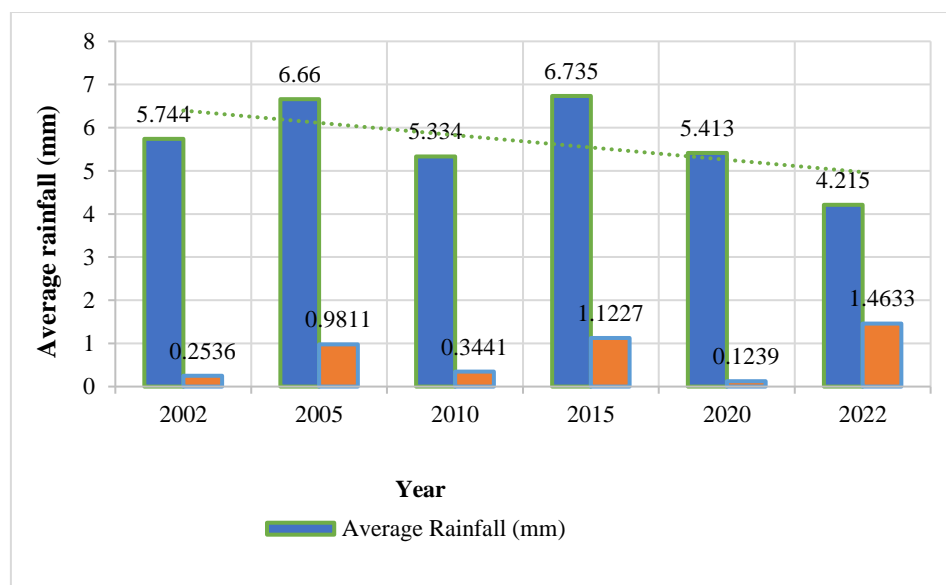


Figure 15: Average rainfall and standard deviation for 2002, 2005, 2010, 2015, 2020, and 2022

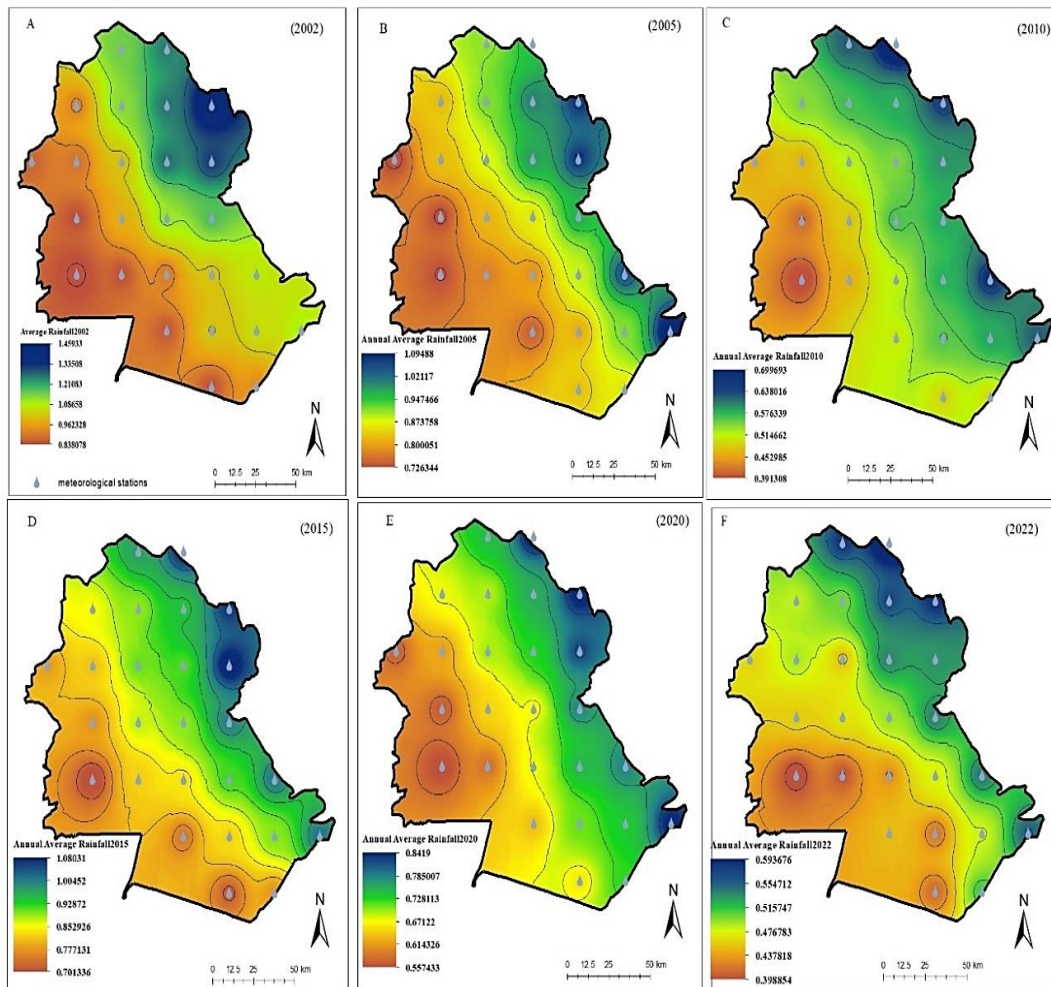


Figure 16: Average rainfall mapping for (a) 2002, (b) 2005, (c) 2010 and (d) 2015, (e)2020, and (f)2022

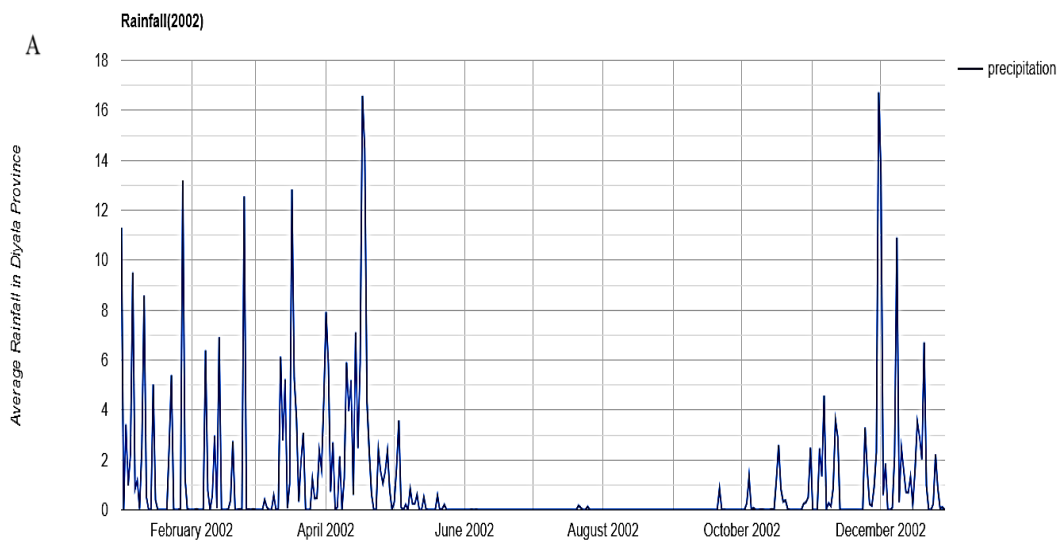


Figure 17: Average Rainfall for years 2002 in Diyala Province

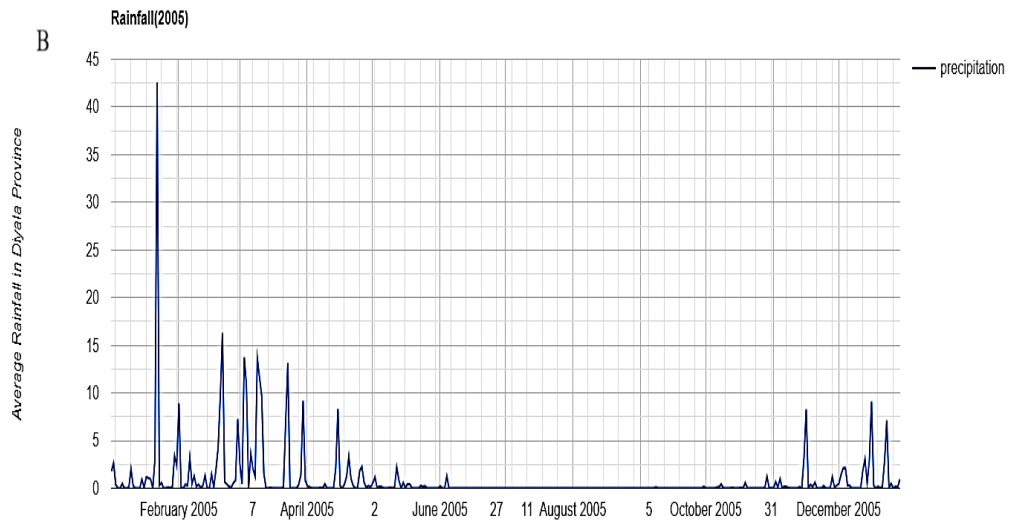


Figure 18: Average Rainfall for the years 2005 in Diyala Province

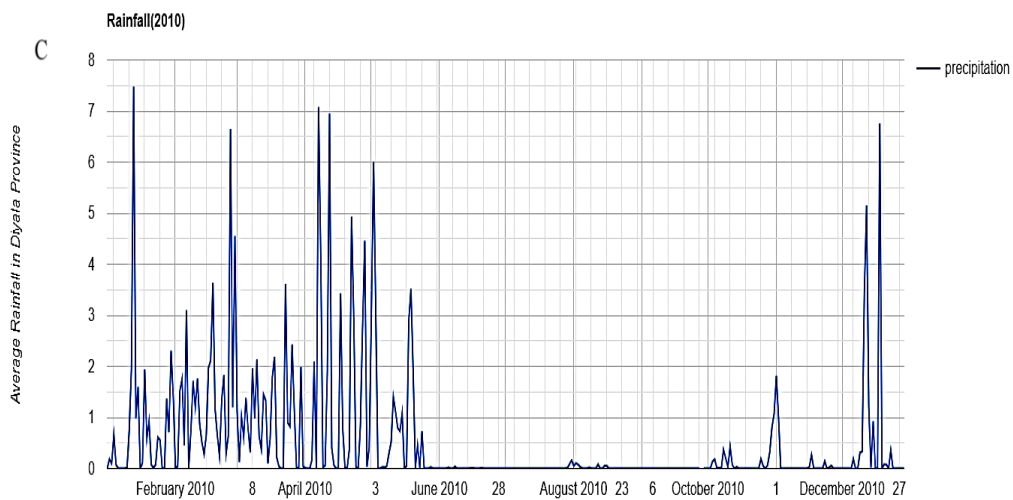


Figure 19: Average Rainfall for years 2010 in Diyala Province

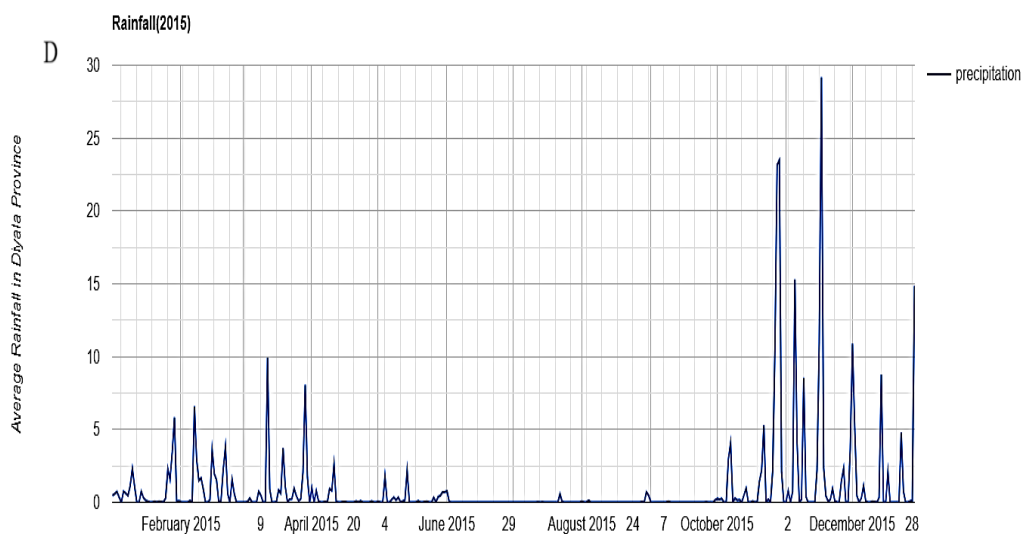


Figure 20: Average Rainfall for years 2015 in Diyala Province

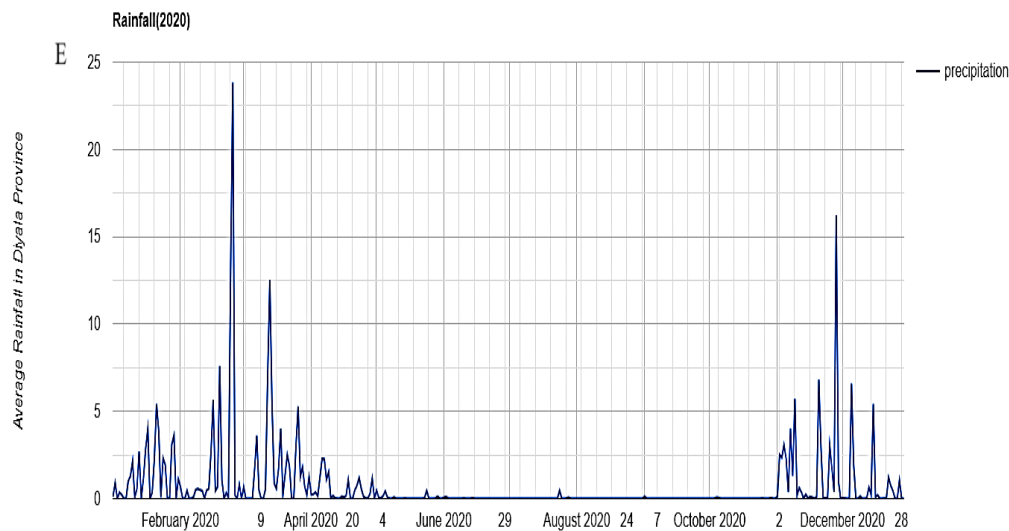


Figure 21: Average Rainfall for the year 2020 in Diyala Province

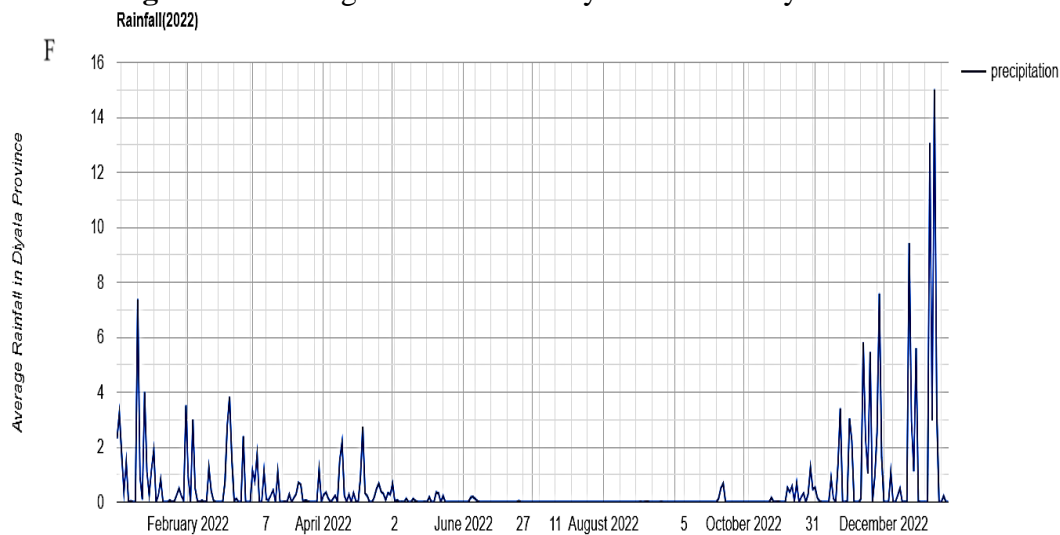


Figure 22: Average Rainfall for years 2022 in Diyala Province

5. Conclusions

This study analyzed drought conditions in Diyala province over twenty years (2002, 2005, 2010, 2015, 2020, and 2022). The study used remote sensing and environmental data to assess drought intensity and soil moisture conditions. VHI results highlight the increasing prevalence of moderate and severe drought, with shifting patterns from 2002, 2005, 2010, 2015, 2020, and 2022. The SMI findings indicate a persistent movement towards drier conditions, with a rise in arid areas and a decrease in wet areas. Average rainfall data emphasizes fluctuating rainfall levels and heightened variability. Drought intensity: the province experienced varying levels of drought throughout the study period. From 2002 to 2022, the area affected by severe drought increased from 66% to 50%, while the area with no drought decreased from 8% to 3%. Soil moisture: the analysis revealed a general trend towards drier conditions. The area classified as "arid" increased from 1.1% in 2002 to 17.1% in 2022. Rainfall: the average annual rainfall showed fluctuations, with some years experiencing lower rainfall amounts than others. The standard deviation of annual rainfall also varied, indicating changes in rainfall variability.

6. Recommendations

These outcomes underscore the pressing need for proactive measures, including sustainable water management, resilient agriculture practices, and public awareness campaigns. Urgent action is essential to address the mounting challenges posed by changing climate patterns, ensuring the resilience and well-being of communities in Diyala Province.

References

- [1] S. Sreekesh, N. Kaur, and S. S. R. Naik, "Agricultural drought and soil moisture analysis using satellite image based indices," *Int. Arch. Photogramm. Remote Sens. Spat. Inf. Sci. - ISPRS Arch.*, vol. 42, no. 3/W6, pp. 507–514, 2019.
- [2] X. Liu, X. Zhu, Y. Pan, S. Li, Y. Liu, and Y. Ma, "Agricultural drought monitoring: Progress, challenges, and prospects," *J. Geogr. Sci.*, vol. 26, no. 6, pp. 750–767, 2016.
- [3] H. A. A. Gaznayee, A. M. Fadhil Al-Quraishi, and A. H. A. Al-Sulttani, "Drought Spatiotemporal Characteristics Based on a Vegetation Condition Index in Erbil, Kurdistan Region, Iraq," *Iraqi J. Sci.*, vol. 62, no. 11, pp. 4545–4556, 2021.
- [4] B. Weare, *Monitoring and Predicting Agricultural Drought: A Global Study*, vol. 5, no. 4, 2006.
- [5] A. M. F. Al-Quraishi, H. A. Gaznayee, and M. Crespi, "Drought trend analysis in a semi-arid area of Iraq based on Normalized Difference Vegetation Index, Normalized Difference Water Index and Standardized Precipitation Index," *J. Arid Land*, vol. 13, no. 4, pp. 413–430, 2021.
- [6] "World Maps of Köppen-Geiger climate classification." [Online]. Available: <http://koeppen-geiger.vu-wien.ac.at/shifts.htm>.
- [7] F. Rubel and M. Kottek, "Observed and projected climate shifts 1901-2100 depicted by world maps of the Köppen-Geiger climate classification," *Meteorol. Zeitschrift*, vol. 19, no. 2, pp. 135–141, Apr. 2010.
- [8] G. Berhan, S. Hill, T. Tadesse, and S. Atnafu, "Using Satellite Images for Drought Monitoring: A Knowledge Discovery Approach," *J. Strateg. Innov. Sustain.*, vol. 7, no. 1, p. 135, 2011.
- [9] R. I. Sholihah *et al.*, "Identification of Agricultural Drought Extent Based on Vegetation Health Indices of Landsat Data: Case of Subang and Karawang, Indonesia," *Procedia Environ. Sci.*, vol. 33, no. December, pp. 14–20, 2016.
- [10] J. Won, J. Seo, J. Lee, O. Lee, and S. Kim, "Vegetation drought vulnerability mapping using a copula model of vegetation index and meteorological drought index," *Remote Sens.*, vol. 13, no. 24, pp. 1–24, 2021.
- [11] A. M. Saleh, "Land Surface Temperature Retrieval of Landsat-8 Data Using Split Window Algorithm-A Case Study of Mosul District," *IOSR J. Agric. Vet. Sci. Ver. II*, vol. 8, no. 2, pp. 2319–2372, 2015.
- [12] R. S. Hameed, L. E. Georg, and B. H. Sayyid, "Modified Vegetation Detection Index Using Different-Spectral Signature," *Iraqi J. Sci.*, vol. 62, no. 11, pp. 4208–4217, 2021.
- [13] M. F. Allawai and B. A. Ahmed, "Using Remote Sensing and GIS in Measuring Vegetation Cover Change from Satellite Imagery in Mosul City, North of Iraq," *IOP Conf. Ser. Mater. Sci. Eng.*, vol. 757, no. 1, p. 012062, Mar. 2020.
- [14] H. A. Atiyah, S. M. Khazael, and A. Q. Makhool, "Spatiotemporal Drought Monitoring Using Remote Sensing Technique in Babel-Iraq," *Iraqi J. Sci.*, pp. 1535–1544, Mar. 2023.
- [15] X. Yang, Y. Chen, and J. Wang, "Combined use of Sentinel-2 and Landsat 8 to monitor water surface area dynamics using Google Earth Engine," *Remote Sens. Lett.*, vol. 11, no. 7, pp. 687–696, 2020.
- [16] S. Basheer *et al.*, "Comparison of Land Use Land Cover Classifiers Using Different Satellite Imagery and Machine Learning Techniques," *Remote Sens.*, vol. 14, no. 19, pp. 1–18, 2022.
- [17] D. S. Al-Khafaji, A. K. Abdulkareem, and Q. Y. Al-Kubaisi, "Rainwater Harvesting Using GIS Technique: A Case Study of Diyala Governorate, Iraq," *Al-Mustansiriyah J. Sci.*, vol. 32, no. 2, pp. 96–102, 2021.
- [18] H. Q. Adeeb and Y. K. Al-Timimi, "Change on detection of vegetation cover and soil salinity using GIS technique in Diyala Governorate, Iraq," *Sci. Rev. Eng. Environ. Sci.*, vol. 30, no. 1, pp. 148–158, 2021.
- [19] C. Funk *et al.*, "The climate hazards infrared precipitation with stations — a new environmental

- record for monitoring extremes,” pp. 1–21, 2015.
- [20] P. Alegre and C. B. Junior, “Alternative methodology to gap filling for generation of monthly rainfall series with GIS approach,” 2018.
- [21] A. N. Abdul-Hammed and A. S. Mahdi, “Monitoring Vegetation Area in Baghdad Using Normalized Difference Vegetation Index,” *Iraqi J. Sci.*, vol. 63, no. 3, 2022.
- [22] H. Hashim, Z. Abd Latif, and N. A. Adnan, “URBAN VEGETATION CLASSIFICATION with NDVI THRESHOLD VALUE METHOD with VERY HIGH RESOLUTION (VHR) PLEIADES IMAGERY,” *Int. Arch. Photogramm. Remote Sens. Spat. Inf. Sci. - ISPRS Arch.*, vol. 42, no. 4/W16, pp. 237–240, 2019.
- [23] “NDVI FAQs: Frequently Asked Questions About The Index.” [Online]. Available: <https://eos.com/blog/ndvi-faq-all-you-need-to-know-about-ndvi/>.
- [24] H. A. A. Gaznayee, A. M. F. Al-Quraishi, K. Mahdi, and C. Ritsema, “A Geospatial Approach for Analysis of Drought Impacts on Vegetation Cover and Land Surface Temperature in the Kurdistan Region of Iraq,” *Water (Switzerland)*, vol. 14, no. 6, 2022.
- [25] D. Jeevalakshmi, S. Narayana Reddy, and B. Manikiam, “Land surface temperature retrieval from LANDSAT data using emissivity estimation,” *Int. J. Appl. Eng. Res.*, vol. 12, no. 20, pp. 9679–9687, 2017.
- [26] K. Saylor, “Landsat 4-7 Level 2 Science Product (L2SP) Guide,” vol. LSDS-1618, no. 4.0. p. 38, 2021.
- [27] USGS, “Landsat Thematic Mapper (TM) Data Format Control Book (DFCB) Landsat Data Format Control Book (DFCB),” vol. LSDS-1336, no. 4.0, 2020.
- [28] K. Saylor and T. Glynn, “Landsat 8-9 Collection 2 Level 2 Science Product Guide | U.S. Geological Survey,” *Landsat 8-9 Collection 2 (C2) Level 2 Science Product (L2SP) Guide*. pp. 1–42, 2022.
- [29] S. T. J. Putro, N. Arif, and T. Sarastika, “Land surface temperature (LST) and soil moisture index (SMI) to identify slope stability,” *IOP Conf. Ser. Earth Environ. Sci.*, vol. 986, no. 1, 2022.
- [30] F. A. Zwain, T. T. Al-Samarrai, and Y. I. Al-Saady, “A Study of Desertification Using Remote Sensing Techniques in Basra Governorate, South Iraq,” *Iraqi J. Sci.*, vol. 62, no. 3, pp. 912–926, Mar. 2021.
- [31] N. Yaa’Cob, Z. N. A. Abd Rashid, N. Tajudin, and M. Kassim, “Landslide Possibilities using Remote Sensing and Geographical Information System (GIS),” *IOP Conf. Ser. Earth Environ. Sci.*, vol. 540, no. 1, pp. 0–9, 2020.
- [32] A. Zuhro, M. P. Tambunan, and K. Marko, “Application of vegetation health index (VHI) to identify distribution of agricultural drought in Indramayu Regency, West Java Province,” *IOP Conf. Ser. Earth Environ. Sci.*, vol. 500, no. 1, 2020.
- [33] A. S. Patil, A. Patil, and S. Panhalkar, “Analysis of the agriculture drought severity and spatial extent using Vegetation Health Index (VHI) in Manganga watershed of Maharashtra, India,” no. February, pp. 35–47, 2021.